

# Microsurgical Anatomy of the Cavernous Sinus: Measurements of the Triangles in and around It

**Gustavo Rassier Isolan, M.D., Ph.D.,<sup>1</sup> Niklaus Krayenbühl, M.D.,<sup>1</sup>  
Evandro de Oliveira, M.D., Ph.D.,<sup>2</sup> and Ossama Al-Mefty, M.D.<sup>1</sup>**

## ABSTRACT

---

**Objectives:** Since the pioneering work of Parkinson, several studies have described the microsurgical anatomy and surgical procedures involving the cavernous sinus (CS). A proposed geometric construct has been adopted as nomenclature for the region by many neurosurgeons. However, authors differ in naming and describing some of these triangular spaces. The purpose of this study is to present the anatomy and measure the dimensions of the 10 triangles in and around this region. **Materials and Methods:** Eighteen CS of five cadaveric heads and four skull bases fixed in formalin were dissected using  $3\times$  to  $40\times$  magnification of the surgical microscope. The heads and skull bases were injected with colored silicone and the sides and area of the triangles were measured. Each cadaveric head was placed in a Sugita head-holder and a cranio-orbitozygomatic approach and a combined extra- and intradural approach were performed. The last step was the detachment of the brain from the skull base and measurement of the inferolateral paraclival and inferomedial paraclival triangles. **Results:** The measurements of the medial border, lateral border, and base of each triangle as well as the standard deviation and area are presented. The posteromedial middle fossa triangle was the largest and the clinoidal triangle the smallest. **Conclusions:** The normal anatomy of the CS triangle and its areas are important in the approach of the CS lesions because these spaces are natural corridors through which the lesions can be reached. The same concept must be used for the triangles around this space. Whenever these geometric spaces might be distorted by pathology or surgical maneuvers, the surgeon must have precise knowledge about their normal sizes.

---

<sup>1</sup>Department of Neurosurgery, University of Arkansas for Medical Sciences, Little Rock, Arkansas; <sup>2</sup>Department of Neurosurgery (Campinas University), Institute of Neurological Sciences, São Paulo-SP, Brazil.

Address for correspondence and reprint requests: Ossama Al-Mefty, M.D., Department of Neurosurgery, University of Arkansas for Medical Sciences, 4301 W. Markham Street, #507,

Little Rock, AR 72205 (e-mail: KeelandAmyE@uams.edu).

Skull Base 2007;17:357-368. Copyright © 2007 by Thieme Medical Publishers, Inc., 333 Seventh Avenue, New York, NY 10001, USA. Tel: +1(212) 584-4662.

Received: February 19, 2007. Accepted: May 18, 2007. Published online: August 7, 2007.

DOI 10.1055/s-2007-985194. ISSN 1531-5010.

**KEYWORDS:** Cavernous sinus, surgical anatomy, triangles, approaches, internal carotid artery

Since the pioneering work of Parkinson,<sup>1,2</sup> several studies have described the microsurgical anatomy and surgical procedures involving the cavernous sinus (CS).<sup>3-19</sup> Parkinson's<sup>1,2</sup> and Dolenc's<sup>3,18,19</sup> descriptions of surgical entry points into the sinus as triangular corridors have been adopted by most surgeons operating in this region. A proposed geometric construct has been adopted as nomenclature for the region by many neurosurgeons. However, authors differ in naming and describing some of these triangular spaces.<sup>15,20-22</sup>

Although numerous articles have reported on the complex anatomy of the CS<sup>3-19</sup> and the dimensions of Parkinson's triangle and the oculomotor triangle have been described previously,<sup>4,9-14</sup> measurements of the other triangles were seldom published in the English literature.<sup>15,22</sup>

The CS is the misnomer of the parasellar space in which the cavernous segment of the internal carotid artery courses and which contains the abducens nerve and sympathetic nerves.<sup>1,23</sup> Its lateral wall contains the third and fourth cranial nerves as well as the first division of the fifth cranial nerve.<sup>3,5,17,24</sup> It is the site of a venous confluence that receives the terminal end of multiple veins draining the orbit, sylvian fissure, and middle and anterior fossa and has free communication with the basilar, superior, and inferior petrosal and intercavernous sinuses.<sup>25</sup> It has five walls: lateral and medial walls, a roof, and posterior and anterior walls and the region in and around it can be divided into 10 triangles: clinoidal, oculomotor, supratrochlear, infratrochlear (Parkinson's), anteromedial middle fossa, anterolateral middle fossa, posterolateral middle fossa (Glasscock's), posteromedial middle fossa (Kawase's), inferolateral paraclival, and inferomedial paraclival.<sup>25</sup>

The purpose of this study is to present the detailed anatomy of the 10 triangles in and around

the CS and to measure the dimensions and area of these triangles.

## MATERIAL AND METHODS

Eighteen CS of five cadaveric heads and four skull bases fixed in formalin were dissected using  $3 \times$  to  $40 \times$  magnification of the surgical microscope. The heads and skull bases were injected with colored silicone and the distances of the sides of the triangles were measured and the area calculated. Each cadaveric head was placed in a Sugita head-holder, turned 30 to 40 degrees, and extended slightly to simulate the surgical position. In the heads, a cranio-orbitozygomatic approach was made according to previous descriptions<sup>24-29</sup> and a combined extra- and intradural approach was performed.<sup>3,19,30</sup> The last step was the detachment of the brain from the skull base and measurement of the inferolateral paraclival and inferomedial paraclival triangles.

The measurement steps of the skull bases were as follows. First, the oculomotor triangle was measured (Fig. 1), followed by creation of a square-shaped dural incision from the middle portion of the lesser sphenoid wing to the planum sphenoidale, exposing the anterior clinoid process, optic canal, planum sphenoidale, and sphenoid edge. The next step was unroofing of the optic canal and drilling of the anterior clinoid process exposing and measuring the clinoidal triangle (Fig. 1). A middle fossa peeling leaving the reticular membrane adherent to the nerves in the lateral wall of the CS was done with every effort to avoid altering the anatomical relationships of the triangles. In this stage the supratrochlear, infratrochlear, anteromedial middle fossa, anterolateral middle fossa (Fig. 1), posterolateral

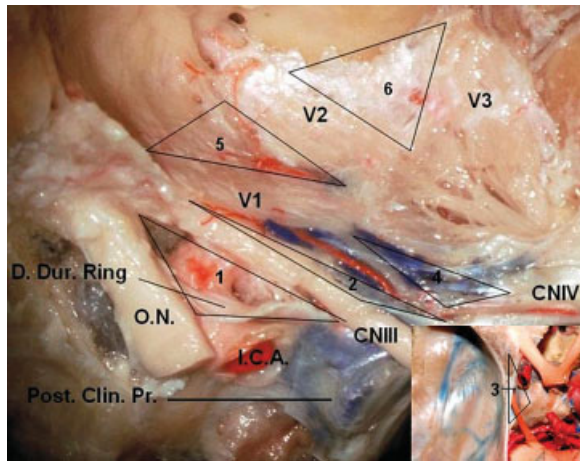


**Figure 1** View of the right cavernous sinus with triangle identification. The anterior clinoid process was removed, exposing the clinoidal triangle (1). The outer layer of the dura has been peeled away, exposing the supratrochlear (2), infratrochlear (4), anteromedial middle fossa (5), and anterolateral middle fossa (6) triangles. The oculomotor triangle (3) is delimited in the smaller picture. The cranial nerve (CN) IV is running parallel to the tentorial artery. D. Dur., distal dural; O.N., optic nerve; I.C.A., internal carotid artery; Post. Clin. Pr., posterior clinoid process.

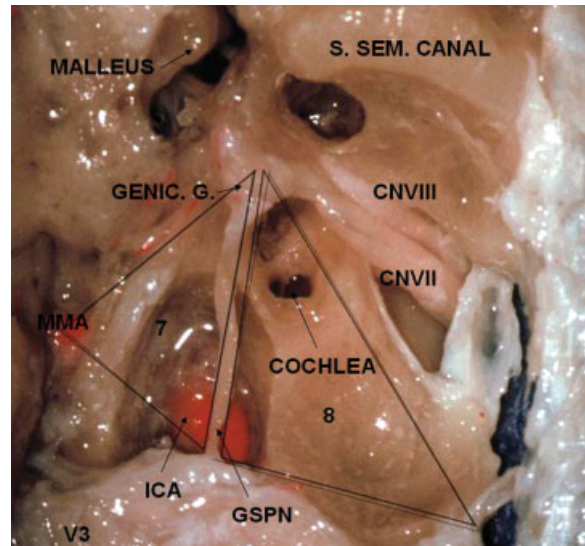


**Figure 2** Superior view of the middle fossa floor showing the anterolateral (7) and anteromedial (8) middle fossa triangles. The bone covering the malleus, ICA, and internal meatus was drilled away. Sup. Sem., superior semicircular; Genic. G., geniculate ganglion; CN, cranial nerve; MMA, middle meningeal artery; ICA., internal carotid artery (intrapetrous portion); GSPN, greater superficial petrosal nerve.

middle fossa, and posteromedial middle fossa triangles (Fig. 2) were measured.

The triangles were measured as follows. In the clinoidal triangle the medial border was defined by the optic nerve confined within the optic canal; the lateral border was a line between the medial aspect of the third cranial nerve from the entry point in the sinus roof lateral to the posterior clinoid process to the point just before entering the superior orbital fissure; and the base corresponded to the dura extending between the posterior limits of the medial and lateral border.

The medial and lateral borders of the supratrochlear were, respectively, the lower surface of the oculomotor nerve and the upper surface of trochlear nerve, and the base was defined by the dura extending between the dural entry points of the third and fourth cranial nerves.

The infratrochlear triangle, known as Parkinson's triangle, was defined by the inferior margin of the trochlear nerve from its beginning in the lateral wall of the CS to the entry point in the

superior orbital fissure (medial border) and by the superior margin of V1 (lateral border). The base was a line connecting the entry points of these nerves into the CS.

The medial border of the oculomotor triangle was defined by a line between the center of the anterior and posterior clinoid processes. The base was the fold of the dura running from the posterior clinoid process to the petrous apex, and the lateral border the fold of dura between the anterior clinoid process and petrous apex.

The anteromedial middle fossa triangle was defined between the lower margin of the ophthalmic nerve (medial border) and the upper margin of the maxillary nerves (lateral border). The base of the triangle was formed by a line connecting the point where the ophthalmic nerve passes through the superior orbital fissure and the maxillary nerves passes through the foramen rotundum.

The anterolateral middle fossa triangle was defined by the lower surface of the maxillary nerve (medial border), the upper surface of the mandibular

nerve (lateral border), and a line connecting the foramen ovale and rotundum (base).

The posterolateral middle fossa triangle, known as Gasscock's triangle, was defined by a line between the points on the lateral surface of the mandibular nerve where the greater petrosal nerve crosses to the foramen spinosum (medial border). The base was formed by the medial margin of the greater petrosal nerve and the lateral border was formed by a line between the foramen spinosum and the center of the geniculate ganglion.

The posteromedial middle fossa triangle, also known as Kawase's triangle, was defined between the lateral margin of the greater petrosal nerve (medial border), the lateral edge of the trigeminal nerve behind the point where the greater petrosal nerve passes below its lateral surface to the crest of the petrous apex (lateral border), and a line along the connection of the posterior border of the mandibular division of the trigeminal nerve and ganglion gasserian (the crest of petrous apex) to the center of the geniculate ganglion (base).

The inferolateral paraclival triangle (Fig. 3) was defined between the intradural entry point of the fourth cranial nerve into the tentorium cerebelli and the entry point of the abducens nerve into Dorello's canal (medial border). The base was defined between the entry points of the trochlear nerve and the petrosal vein into the superior petrosal sinus. The lateral border was defined between the entry point of the abducens nerve and petrosal vein.

The inferomedial paraclival triangle (Fig. 3) was defined above by a line extending from the posterior clinoid process to the dural entrance of the trochlear nerve (base), laterally by a line connecting the dural entrance of the trochlear and abducens nerves (lateral border), and medially by a line extending from the dural entrance of the abducens nerve to the posterior clinoid process (medial border). The schematic view of the triangle's limits is seen in Table 1.

The area of a triangle is  $S = \frac{1}{2}bh$ , where  $b$  is the length of any side of the triangle (the *base*) and  $h$  (the *height*) is the perpendicular distance

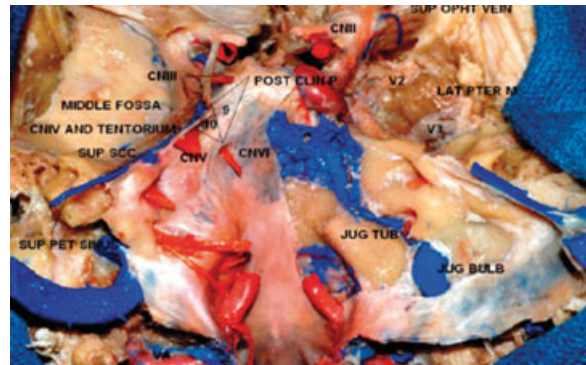


**Figure 3** Posterior view of the inferomedial paraclival (9) and inferolateral paraclival (10) triangles. The dura in the right clivus was peeled away. Jug. Tub., jugular tubercle; CN, cranial nerve; Post. Clin. P., posterior clinoid process; Lat. Pter. M., lateral pterygoid muscle; Sup. Ophth., superior ophthalmic; Sup. Pet., superior petrosal; Sup. SCC., superior semicircular canal.

between the base and the vertex not on the base. The Hero's formula was used in the following way: given the lengths of the sides  $a$ ,  $b$ , and  $c$  and the semiperimeter

$$S = \frac{1}{2} (a + b + c)$$

$$\Delta = \sqrt{s(s-a)(s-b)(s-c)}$$

## RESULTS

The results are shown in Table 2.

The posteromedial middle fossa triangle was the largest and the clinoidal triangle the smallest.

Figs. 4 and 5 show important anatomical structures related to the CS triangles and Figs. 6 and 7 show the relation between the CS triangles and adjacent skull base regions.

## DISCUSSION

A precise knowledge of the CS microanatomy is paramount. Although CS lesions (neoplastic or

**Table 1** Limits of the Triangles in and around the Cavernous Sinus

Triangle	Medial Border	Lateral Border	Base
Clinoidal	CN II	CN III	Line between posterior limit of medial and lateral border
Supratrochlear	CN III	CN IV	Line between posterior limit of medial and lateral border
Oculomotor	Interclinoid fold	Anterior petroclinoid fold	Posterior petroclinoid fold
Infratrochlear	CN IV	V1	Line between posterior limit of medial and lateral border
Anteromedial middle fossa	V1	V2	Line between the anterior limit of medial and lateral border
Anterolateral middle fossa	V2	V3	Line between the anterior limit of medial and lateral border
Posterolateral middle fossa	Line between where the GSPN crosses under V3 and the foramen spinosum	Line between the foramen spinosum and geniculate ganglion	GSPN
Posteromedial middle fossa	GSPN	Line between where the GSPN crosses under V3 and the petrous apex	Line between the crest of the petrous apex to the geniculate ganglion
Inferomedial paraclival	Line between the posterior clinoid process and the entry point of the CN VI at Dorello's canal	Line between the entry point of CN IV at the tentorium and CN VI at Dorello's canal	Line between the posterior clinoid process and the entry point of the of CN IV at the tentorium
Inferolateral paraclival	Line between the entry point of CN IV at the tentorium and CN VI at Dorello's canal	Line between entry point of CN VI at Dorello's canal and the superior petrosal vein at the superior petrosal sinus	Line between entry point of CN IV at the tentorium and the superior petrosal vein at the superior petrosal sinus

CN, cranial nerve; GSPN, greater superficial petrosal nerve.

vascular) distort the normal anatomy, a guiding knowledge in the normal anatomy is indispensable to recognizing this distortion. Despite some cases of CS neoplasm that might develop a large degree of anatomical distortion,<sup>24</sup> dissection of anatomic entry corridors is not significantly affected in intracavernous aneurysms in terms of accurate identification of critical landmarks. Also, the surgeon must keep in mind that the triangles can be enlarged by the mobilization of the cranial nerves.

Regarding the method used by the authors, there are three topics that must be discussed, two

concerning measurements and one concerning nomenclature. All measurements were performed by one of the authors (GRI) to avoid bias. The Hero's formula makes for an easy calculation of the area of a triangle when all three sides are known. In relation to the nomenclature of the triangles, the authors used the system adopted by Rhoton.<sup>25</sup>

The clinoidal triangle contains the optic strut anteriorly, the subclinoidal segment of the ICA in the middle, and the roof of the CS posteriorly, which are exposed after drilling of the anterior clinoid process (Fig. 1). Sometimes a mucous

**Table 2** Dimensions of the 10 Triangles in and around the Cavernous Sinus\*

Triangle	Medial Border	Lateral Border	Base	Area
Clinoidal	7.34 ± 0.49	13.89 ± 0.74	8.53 ± 0.51	26.25 ± 5.6
Supratrochlear	13.18 ± 3.19	14.27 ± 1.35	5.51 ± 0.82	36.46 ± 4.34
Oculomotor	12.38 ± 0.63	17.23 ± 0.53	11.35 ± 0.86	69.24 ± 8.99
Infratrochlear	10.29 ± 0.99	12.33 ± 1.19	4.34 ± 0.44	21.06 ± 4.56
Anteromedial middle fossa	10.18 ± 0.62	7.87 ± 0.29	9.96 ± 1.13	36.26 ± 3.75
Anterolateral middle fossa	12.25 ± 0.67	11.59 ± 1.61	10.80 ± 1.12	51.52 ± 4.25
Posterolateral middle fossa	14.71 ± 1.16	7.04 ± 0.47	15.33 ± 0.82	49.25 ± 5.23
Posteromedial middle fossa	14.04 ± 0.79	14.82 ± 0.59	17.18 ± 1.92	97.69 ± 8.13
Inferomedial paraclival	16.22 ± 0.36	11.37 ± 0.54	7.25 ± 1.03	41.79 ± 6.45
Inferolateral paraclival	11.37 ± 0.54	14.94 ± 1.33	7.86 ± 1.37	34.88 ± 8.25

\*The dimensions of each side of the triangle (media) are in mm and the area in mm<sup>2</sup>. The symbol ± corresponds to the standard deviation.

membrane of the sphenoidal sinus can be exposed anteriorly. The venous plexus that surrounds this part of the ICA can vary in length. Sometimes it reaches only the carotid oculomotor membrane becoming in this part extracavernous.<sup>24</sup> There is a fibrous tissue in the medial surface of the oculomotor nerve that divides, according to Dolenc, "the extra-parasellar space from parasellar space compartments."<sup>3</sup> Day<sup>22</sup> and Fukushima<sup>20</sup> described the space that exposes the clinoidal segment of this ICA as anterior triangle, which is defined by the lateral border of the intracanalicular optic nerve, the medial wall of the superior orbital fissure dura, and the dural ring surrounding the ICA as it enters the subarachnoid space. They found, with this definition, the following measurements: posterior border averaged 6.30 mm (range, 5 to 8 mm), medial border averaged 6.88 mm (range, 4.5 to 9 mm), and the lateral border averaged 8.72 (range, 6.5 to 9.8 mm). However, using the same morphometric parameters of our research and Dolenc<sup>3</sup> and defining this space as the anteromedial triangle, the average of the measurements of Watanabe et al<sup>15</sup> of the medial border, lateral border, and base were, respectively, 9.5, 13.3, and 7.2 mm. The anterior clinoidal process can be pneumatized, communicating with the sphenoidal sinus. The subclinoidal ICA sometimes is surrounded by an osseous bridge between the anterior and middle clinoid process (caroticoclinoidal foramen); in these cases, remov-

ing this process in one piece can damage the ICA.<sup>17</sup> The epidural removal is recommended, but there have been cases of such a meningioma invading the anterior clinoid process. This structure becomes thick and elongated and intradural removal is necessary.<sup>21</sup>

The oculomotor triangle is where the oculomotor nerve enters the roof of the CS. The corners of this space are the anterior and posterior clinoid process and the petrous apex. In these points are connected the anterior and posterior petroclinoid and the interclinoid dural fold. This space exposes the distal intracavernous carotid artery and is an important access corridor for tumor involving the medial CS and for approaches to the interpeduncular fossa. In the Watanabe study, measurements of the medial border, lateral border, and base were, respectively 10.4, 16.1, and 12.2 mm. The medial triangle is the name give by some authors who consider the following corners: subclinoidal carotid segment, posterior clinoid process, and the porus oculomotorius.<sup>22</sup> The mean dimensions found by Umansky and Nathan were 9.6 × 16.6 × 13.8 mm.<sup>31</sup>

The supratrochlear triangle is between the oculomotor and trochlear nerves and opening it can expose the posterior bend of the intracavernous carotid artery and the meningo-hypophyseal trunk origin,<sup>22</sup> whenever the origin of this trunk is more commonly related from the Parkinson's triangle.<sup>4,25</sup> In addition, the inferolateral trunk can be identified

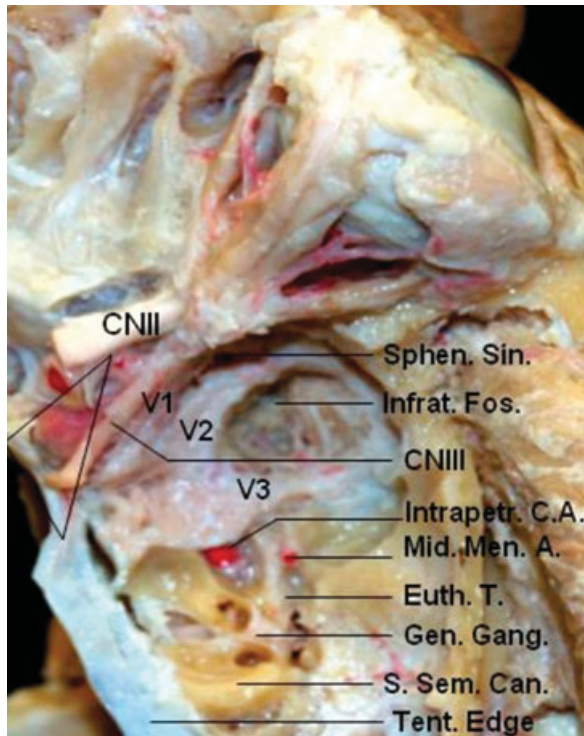


**Figure 4** Superior view of the middle fossa structures. After drilling bone between V2 and V3 it is possible to identify the superior head of the lateral pterygoid muscle in the infratemporal fossa. The clinoidal triangle is delimited. Sphen. Sin., sphenoid sinus; Infrat. Fos., infratemporal fossa; CN, cranial nerve; Intrapetr. C. A., intrapetrous carotid artery; Mid. Men. A., middle meningeal artery; Eust. T., Eustachian tube; Gen. Gang., geniculate ganglion; S. Sem. Can., superior semicircular canal; Tent., tentorial.

inside this triangle and, less commonly, the medial loop of the ICA.<sup>3</sup> The nerves that constitute this triangle cross over the oculomotor nerve before entering into the superior orbital fissure. It is possible to recognize that the nerves that supply the extraocular muscle are irrigated by the inferolateral trunk.<sup>3,7</sup> Paramedial triangle is the other name of this space.<sup>3</sup>

The infratrochlear triangle, also known as Parkinson's triangle, is bounded by the trochlear nerve and the ophthalmic division of the trigeminal nerve. Generally the meningo-hypophyseal trunk from the posterior bend of the ICA is located at this triangle, except if the artery is elongated and tortuous. In this case the origin may be pushed

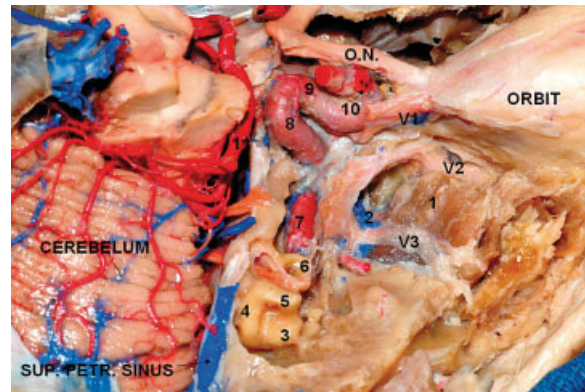


**Figure 5** Superior view of the middle fossa structures and portions of the internal carotid artery. The tentorium was removed, exposing the cerebellum. The temporal fossa floor was partially drilled out, exposing the lateral pterygoid muscle in the infratemporal fossa. The gasserian ganglion was removed as well as the roof and lateral wall of the orbit. 1, lateral pterygoid muscle (upper head) in the infratemporal fossa; 2, pterygoid venous plexus; 3, lateral semicircular canal; 4, posterior semicircular canal; 5, superior semicircular canal; 6, cochlea; 7, internal carotid artery (intrapetrous portion); 8, internal carotid artery (intracavernous portion); 9, meningo-hypophyseal trunk; 10, internal carotid artery (subclinoidal portion). Sup. Petr., superior petrosal; O.N., optic nerve.

upward.<sup>25</sup> The sixth nerve can be exposed through this triangle.<sup>3</sup> It was originally described by Parkinson for direct entry into the CS.<sup>1,23</sup> Rhoton et al found the medial border average to be 13 mm (range, 8 to 20 mm), the lateral border averaged 14 mm (range, 5 to 24 mm), and the posterior border average was 6 mm (range, 3 to 14 mm),<sup>4</sup> but there were triangular spaces not large enough to provide a good surgical exposure. However, this space can be enlarged by dissecting and displacing V1 and the fourth nerve.<sup>3</sup> Lateral triangle is the name of this space given by some authors.<sup>15,22</sup> The other mean dimensions reported previously were 17 × 17 × 5 mm,<sup>10</sup> 12 × 13 × 4 mm,<sup>9</sup> 10.48 × 11.79 × 6.94 mm,<sup>22</sup> and 13.9 × 15.5 × 7.6 mm.<sup>15</sup>

The anteromedial middle fossa triangle, first described by Mullan,<sup>32</sup> is situated between the ophthalmic and maxillary nerves. Displacing V1 medially exposes the sixth nerve and the ICA. There is fatty tissue in the anterior part of this

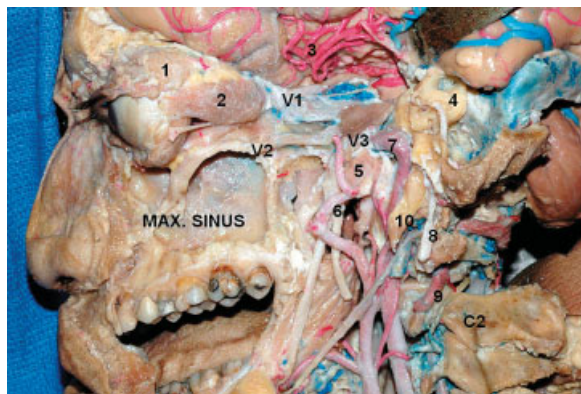


**Figure 6** Lateral view of the CS and adjacent regions. The lateral and anterior walls of the maxillary sinus were removed. The walls of the orbit and orbital fat were removed. The temporal lobe is displaced posteriorly to expose the CS. The dura of the middle fossa was peeled away and the bone of the middle fossa floor was drilled out to show the anatomical relationship between the temporal and infratemporal fossa structures. Mastoidectomy was performed, preserving the mastoid tip. 1, lacrimal gland; 2, rectus lateralis muscle; 3, middle cerebral artery; 4, otic capsule (semicircular canals); 5, Eustachian tube; 6, middle meningeal artery; 7, internal carotid artery (intrapetrous portion); 8, facial nerve; 9, vertebral artery; 10, styloid process. CS, cavernous sinus; Max., maxillary.

space that can be an extension of periorbital fat.<sup>3</sup> Removing bone in this triangle will expose the sphenoid sinus. The average of this space, also known as the anterolateral triangle<sup>3,15,22</sup> by Day and Watanabe, of the medial border, lateral border, and base were, respectively, 10.63 and 11.7 mm, 10.36 and 7.8 mm, 5.83 and 12.0 mm.<sup>15,22</sup>

The anterolateral middle fossa triangle is bounded by the second and third divisions of the trigeminal nerve, V3 being shorter than V2. It is called the far-lateral<sup>22</sup> or lateral triangle.<sup>3,15</sup> The sphenoidal emissary foramen, in some cases, is located in this space joining the CS with the pterygoid venous plexus. Anterolateral extensions of intracavernous tumors are exposed through this triangle. Retracting its posterior corner can expose the intrapetrous ICA. Opening the bone in the medial wall of this space exposes in some cases the lateral wall of the sphenoid sinus. The measurements of Day and Watanabe of the medial border, lateral border, and base were, respectively, 10.03

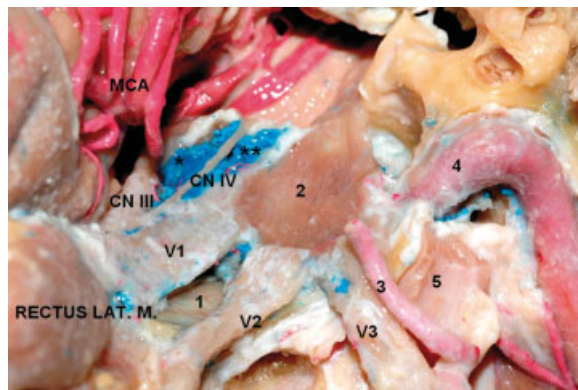


**Figure 7** Middle fossa floor and cavernous sinus. 1, sphenoidal sinus; 2, gasserian ganglion; 3, middle meningeal artery; 4, internal carotid artery (intrapetrous portion); 5, Eustachian tube. Lat. M., lateralis muscle; MCA, middle cerebral artery; \*supratrochlear triangle; \*\*infratrochlear triangle.

and 13.9 mm, 7.54 and 15.5 mm, and 10.53 and 7.6 mm.

The posterolateral middle fossa triangle or posterolateral triangle<sup>3,15</sup> was defined by Glasscock originally with the corners being the posterior rim of the foramen ovale, the apex of the cochlea, and the posterior border of the mandibular division of the trigeminal nerve.<sup>24</sup> Rhoton defines this space by the lateral surface of the mandibular nerve distal to the point at which the greater petrosal nerve crosses below the lateral surface of the trigeminal nerve and by the anterior margin of the greater petrosal nerve.<sup>25</sup> We considered the medial border being the greater petrosal nerve, the anterior border being the trigeminal nerve and its mandibular division, but the lateral border, contrary to the Watanabe's<sup>15</sup> and Dolenc's<sup>3</sup> measurements (arcuate eminence of the petrous bone),<sup>15</sup> being the distance between the point at which the greater petrosal nerve crosses below the lateral surface of the trigeminal nerve and the center of the geniculate ganglion. In our opinion, these parameters are more precise for reproducibility than the arcuate eminence. Portions of the posterior and lateral loops of the ICA can be exposed through this triangle, as well as the greater and lesser petrosal nerves, the tensor tympani muscle, the Eustachian tube, and



the middle meningeal artery.<sup>3</sup> Drilling its floor exposes the infratemporal fossa. In the Day measurements<sup>22</sup> the average length of the medial border was bigger than our and Watanabe's<sup>15</sup> measurements showed, and the lateral border was lesser, probably because the anatomical points were different among these authors.

The posteromedial middle fossa triangle, also known as Kawase's triangle, Kawase-Shiobara's triangle, or the posteromedial triangle, is defined by the porus trigeminus, the cochlea, and the mandibular division of the trigeminal nerve.<sup>22,24</sup> Rhoton defined one of the sides as the line between the hiatus fallopii to the dural ostium of Meckel's cave.<sup>25</sup> We consider the posterior border to be a line between the posterior border of the mandibular division of the trigeminal nerve and the center of the geniculate ganglion, according to the exposure described above. This triangle may be removed for entry into the posterior CS and as an entry point to the posterior fossa through the petrous apex (anterior petrosectomy). Drilling the lateral apex of this triangle exposes the cochlea. The petrous carotid crosses the anterior margin of this triangle and the proximal control of this vessel can be achieved here.

The inferolateral paraclival triangle has the follows corners, entry sites of the trochlear and abducens nerves, and the site where the first petrosal vein joins to the superior petrosal sinus. Day considers this space (the posteroinferior triangle) bounded by the porus trigeminalis, the entrance of the sixth nerve in Dorello's canal, and the fourth cranial nerve entrance along the incisura into the lateral wall of the CS.<sup>22</sup> The authors have adopted the definition of Dolenc, who, in addition, divides this space by a line between the entry point of the petrosal vein and the anterior limit of the entry point of the fifth cranial nerve, in the "tentorial triangle" and "osseous triangle"<sup>3</sup> above and below the fifth nerve, respectively. The first contains the tentorial artery, also known as the Bernasconi-Cassinari artery, the superior petrosal sinus, and the tentorium superior and posterior to Meckel's cave. The osseous triangle corresponds to Kawase's

triangle in the middle fossa and contains the entry point of the fifth nerve.

The inferomedial paraclival triangle is bounded by the posterior clinoid process, the dural entrance of the trochlear and abducens nerve. This space extends in the posterior sinus wall. The lateral edge of the dorsum sellae, petroclival fissure, and Dorello's canal can be exposed after drilling of the medial part of this space. The contents of this triangular space are the abducens nerve, the posterior genu of the ICA, the dorsal meningeal artery, the basilar venous plexus, and the posterior petroclinoid fold.<sup>3,33</sup>

While some authors do not describe all the spaces mentioned above, others<sup>22,24</sup> consider another two spaces: the pre- and postmeatal spaces. The premeatal space is defined by the intrapetrous carotid genu, the geniculate ganglion, and the medial lip of the porus acusticus and is used to locate the cochlea during extradural drilling of the medial fossa. The postmeatal triangle is bounded by the internal auditory canal, superior semicircular canal, and the petrous ridge.

Details of different ways to approach the CS are described in the literature.<sup>34-40</sup>

## CONCLUSION

The normal anatomy of the CS triangles (clinoidal, oculomotor, supratrochlear, and infratrochlear), as well as their dimensions, are important for approaches of CS lesions because these spaces are natural corridors through which lesions inside the CS can be reached. The same concept must be applied to the triangles around this space, such as the four middle fossa triangles (anteromedial, anterolateral, posterolateral, and posteromedial middle fossa) and two paraclival triangles (inferolateral and inferomedial paraclival). The largest triangle is the posteromedial middle fossa triangle and the smallest is the clinoidal triangle. Whenever this space might be distorted by pathology and even moreso by

surgical maneuvers, the surgeon must have a precise idea about the sizes of these spaces.

## REFERENCES

- Parkinson D. A surgical approach to the cavernous portion of the carotid artery: anatomical studies and case report. *J Neurosurg* 1965;23:474–483
- Parkinson D. Transcavernous repair of carotid cavernous fistula. Case report. *J Neurosurg* 1967;26:420–424
- Dolenc VV. *Microsurgical Anatomy and Surgery of the Central Skull Base*. Wien, Austria: Springer-Verlag; 2003
- Harris FS, Rhoton AL Jr. Anatomy of the cavernous sinus: a microsurgical study. *J Neurosurg* 1976;45:169–180
- Inoue T, Rhoton AL Jr, Theele D, Barry ME. Surgical approaches to the cavernous sinus: a microsurgical study. *Neurosurgery* 1990;26:903–932
- Isolan G, de Oliveira E, Mattos JP. The arterial compartment of cavernous sinus: analysis of 24 cavernous sinus. *Arq Neuropsiquiatr* 2005;63:259–264
- Krisht A, Barnett DW, Barrow DL, Bonner G. The blood supply of the intracavernous cranial nerves: an anatomic study. *Neurosurgery* 1994;34:275–279
- Kawase T, Van Loveren HR, Keller JT, Tew JM Jr. Meningeal architecture of the cavernous sinus: clinical and surgical implications. *Neurosurgery* 1996;39:527–536
- Miyazaki Y, Yamamoto I, Shinozuka S, Sato O. Microsurgical anatomy of the cavernous sinus. *Neurol Med Chir (Tokyo)* 1994;34:150–163
- Sekhar LN, Burgess J, Akin O. Anatomical study of the cavernous sinus emphasizing operative approaches and related vascular and neural reconstruction. *Neurosurgery* 1987;21:806–816
- Seoane E, Rhoton AL, de Oliveira E. Microsurgical anatomy of the dural carotid collar (carotid collar) and rings around the clinoid segment of the internal carotid artery. *Neurosurgery* 1998;42:869–886
- Spektor S, Piontek E, Umansky F. Orbital venous drainage into the anterior cavernous sinus space: microanatomic relationships. *Neurosurgery* 1997;40:532–540
- Taptas JN. The so-called cavernous sinus: a review of the controversy and its implications for neurosurgeons. *Neurosurgery* 1982;11:712–717
- Umansky F, Valarezzo A, Elidan J. The superior wall of the cavernous sinus: a microanatomical study. *J Neurosurg* 1994;81:914–920
- Watanabe A, Nagaseki Y, Ohkubo S, et al. Anatomical variations of the ten triangles around the cavernous sinus. *Clin Anat* 2003;16:9–14
- Yasuda A, Campero A, Martins C, Rhoton AL Jr, Ribas GC. The medial wall of the cavernous sinus: microsurgical anatomy. *Neurosurgery* 2004;55:179–190
- Yasuda A, Campero A, Martins C, Rhoton AL, de Oliveira E, Ribas GC. Microsurgical anatomy and approaches to the cavernous sinus. *Neurosurgery* 2005;56:4–27
- Dolenc V. Direct microsurgical repair of intracavernous vascular lesions. *J Neurosurg* 1983;58:824–831
- Dolenc VV. A combined epi- and subdural direct approach to carotid-ophthalmic artery aneurysms. *J Neurosurg* 1985;62:667–672
- Fukushima T. Direct operative approach to the vascular lesions in the cavernous sinus: summary of 27 cases. *Mt Fuji Workshop. Cerebrovasc Dis* 1988;6:169–189
- Al-Mefty O. *Operative Atlas of Meningeomas*. Philadelphia: Lippincott-Raven; 1998
- Day JD. *Microsurgical Dissection of the Cranial Base*. New York: Churchill Livingstone; 1996
- Parkinson D. Collateral circulation of cavernous carotid artery: anatomy. *Can J Surg* 1964;7:251–268
- Al-Mefty O. *Surgery of the Cranial Base*. Boston: Kluwer Academic Publishers; 1989
- Rhoton AL Jr. The supratentorial cranial space: microsurgical anatomy and surgical approaches. *Neurosurgery* 2002;21(suppl 1):375–410
- Al-Mefty O. Supraorbital-pterional approach to skull base lesions. *Neurosurgery* 1987;21:474–477
- Eisenberg MB, Al-Mefty O, DeMonte F, Burson GT. Benign nonmeningeal tumors of the cavernous sinus. *Neurosurgery* 1999;44:949–954
- Al-Mefty O, Smith RR. Surgery of tumors invading the cavernous sinus. *Surg Neurol* 1988;30:370–381
- DeMonte F, Smith HK, Al-Mefty O. Outcome of aggressive removal of cavernous sinus meningiomas. *J Neurosurg* 1994;81:245–251
- Dolenc VV. Approaches to and techniques of surgery within the cavernous sinus. In: Torrens M, Al-Mefty O, Kobayashi S, eds. *Operative Skull Base Surgery*. New York: Churchill Livingstone; 1997:207–236
- Umansky F, Nathan H. The lateral wall of the cavernous sinus with special reference to the nerves related to it. *J Neurosurg* 1982;56:228–234
- Mullan S. Treatment of carotid-cavernous fistulas by cavernous sinus occlusion. *J Neurosurg* 1979;50:131–144
- Destrieux C, Velut S, Kakou MK, Lefrancq T, Arbeille B, Santini J. A new concept in Dorello's canal microanatomy: the petroclival venous confluence. *J Neurosurg* 1997;87:67–72
- Hakuba A, Tanaka K, Suzuki T, Nishimura S. A combined orbitozygomatic infratemporal epidural and subdural approach for lesions involving the entire cavernous sinus. *J Neurosurg* 1989;71:699–704
- De Jesús O, Sekhar LN, Parikh HK, Wright DC, Wagner DP. Long-term follow-up of patients with meningiomas involving the cavernous sinus: recurrence, progression, and quality of life. *Neurosurgery* 1996;39:915–920
- Kawase T, Taya S, Shiobara R, Mine T. Transpetrosal approach for aneurysms of the lower basilar artery. *J Neurosurg* 1985;63:857–861

37. Marinkovic S, Gibo H, Vucevic R, Petrovic P. Anatomy of the cavernous sinus region. *J Clin Neurosci* 2001;8(suppl 1): 78–81
38. Sekhar LN, Moller AR. Operative management of tumors involving the cavernous sinus. *J Neurosurg* 1986;64:879–889
39. Tedeschi H, de Oliveira EP, Wen HT, Rhoton AL. Perspectives on the approaches to lesions in and around the cavernous sinus. *Oper Tech Neurosurg* 2001;4:82–107
40. Krayenbühl N, Isolan GR, Hafez A, Yasargil MG. The relationship of the fronto-temporal branches of the facial nerve to the fascias of the temporal region: a literature review applied to practical anatomical dissections. *Neurosurg Rev* 2007;30:8–15